Geomechanics and Engineering, *Vol. 30, No. 5 (2022) 401-411*
https://doi.org/10.12989/gae.2022.30.5.401

Dynamic failure features and brittleness evaluation of coal under different confining pressure

Xiaohui Liu*[1,2,3], Yu Zheng[4], Qijun Hao[3], Rui Zhao[1,2], Yang Xue[5] and Zhaopeng Zhang[3]

[1]*Key Laboratory of Fluid and Power Machinery, Ministry of Education, Xihua University, Chengdu, 610039, China*
[2]*School of Energy and Power Engineering, Xihua University, Chengdu, 610039, China*
[3]*Key Laboratory of Deep Earth Science and Engineering, Sichuan University, Ministry of Education, Chengdu, 610065, China*
[4]*Southwest Municipal Engineering Design & Research Institute of China, Chengdu, 610081, China*
[5]*CHN Energy Dadu River Hydropower Development Co., Ltd, Chengdu 610041, China*

(*Received October 24, 2020, Revised June 7, 2022, Accepted July 12, 2022*)

Abstract. To obtain the dynamic mechanical properties, fracture modes, energy and brittleness characteristics of Furong Baijiao coal rock, the dynamic impact compression tests under 0, 4, 8 and 12 MPa confining pressure were carried out using the split Hopkinson pressure bar. The results show that failure mode of coal rock in uniaxial state is axial splitting failure, while it is mainly compression-shear failure with tensile failure in triaxial state. With strain rate and confining pressure increasing, compressive strength and peak strain increase, average fragmentation increases and fractal dimension decreases. Based on energy dissipation theory, the dissipated energy density of coal rock increases gradually with growing confining pressure, but it has little correlation with strain rate. Considering progressive destruction process of coal rock, damage variable was defined as the ratio of dissipated energy density to total absorbed energy density. The maximum damage rate was obtained by deriving damage variable to reflect its maximum failure severity, then a brittleness index BD was established based on the maximum damage rate. BD value declined gradually as confining pressure and strain rate increase, indicating the decrease of brittleness and destruction degree. When confining pressure rises to 12 MPa, brittleness index and average fragmentation gradually stabilize, which shows confining pressure growing cannot cause continuous damage. Finally, integrating dynamic deformation and destruction process of coal rock and according to its final failure characteristics under different confining pressures, BD value is used to classify the brittleness into four grades.

Keywords: average fragmentation; brittleness index; dissipated energy density; maximum damage rate; split Hopkinson pressure bar

1. Introduction

With growing demand for coal resources, the depth and intensity of coal mining increase gradually. As mining depth increases, coal rock failure feature changes from brittle to plastic under confining pressure effect. During dynamic excavation of coal mines, redistribution of surrounding rock stress often leads to dynamic disasters such as impact instability. Therefore, studying the mechanical behavior, failure mechanism and brittleness characteristics of coal rock under dynamic loading can provide scientific guidance for safe and efficient coal mining.

On the study of mechanical properties and failure characteristics of rocks under dynamic loading, many scholars have carried out impact compression tests on different rocks by using SHPB (Demirdag *et al*. 2010, Al-Salloum *et al*. 2014), and found that the strength, deformation parameters and failure characteristics of rock are closely related to strain rate and confining pressure. For example, Omidvar *et al*. (2012) conducted dynamic compression tests on sand and pointed out its compressive strength improves with increasing strain rate and confining pressure. Gong *et al*. (2019) indicated that the failure mode of sandstone under dynamic impact varies from tensile failure to shear failure as confining pressure increases, which has obvious brittle-ductile transition characteristics. The deformation and destruction of rock is actually a process of energy dissipation and energy release (Bernabe and Revil 1995, Stefer *et al*. 2003). And Kim *et al*. (2018) analyzed the effects of loading rate on rock fragmentation and energy absorption. For coal rock, its mechanical parameters present significant strain rate correlation and confining pressure effect, and the failure mode shows obvious brittle-ductile transition characteristics as strain rate and confining pressure increases (Lu *et al*. 2019). The distribution characteristics of coal rock fragments after macroscopic failure have obvious self-similarity, and fractal dimension can properly characterize its broken degree(Xie *et al*. 1996). Liu *et al*. (2015) used fractal dimension to reflect the fracture degree of coal under impact loading, and deeply analyzed its failure characteristics. Energy dissipation is the cause of rock fracture and eventual failure, and Feng *et al*. (2016) stated that the greater energy dissipation under dynamic loading, the smaller coal rock fragment would be after destruction. It can be found that many researches on rock dynamic properties only consider

*Corresponding author, Associate Professor
E-mail: liuxh@mail.xhu.edu.cn

ISSN: 2005-307X (Print), 2092-6219 (Online)

(a) SHPB test platform (b) Confining pressure device

Fig. 1 SHPB test device

one aspect of mechanical properties, failure mode or energy evolution law. Thus, under the coupling action of confining pressure and strain rate, studying the dynamic properties of coal rock from different aspects is meaningful.

At the same time, rock impact instability during dynamic excavation is essentially a process of brittle failure, so studying rock brittleness features is significant. Rock brittleness can be characterized by brittleness index. However, the definition methods of brittleness index are different, scholars have summarized more than 30 kinds of brittleness index (Hucka and Das 1974, Özfırat *et al*. 2016, Ghadernejad *et al*. 2020). For instance, it can be established through stress-strain curve (Rybacki *et al*. 2016), deformation parameters (Moska *et al*. 2018), energy evolution traits (Munoz *et al*. 2016), etc. Further, confining pressure and strain rate have a certain influence on the brittleness of rock, which can be reflected in the change of brittleness index (Meng *et al*. 2015). Zhou *et al*. (2020) introduced brittleness index *BI* based on statistical damage model, and used *BI* value to analyze brittle-ductility transition of rock under different confining pressures. Moreover, rock brittleness degree can be classified by brittleness index. Yagiz (2009) established the brittleness index *BIM*, then classified rock into six grades from brittleness to ductility. Kivi *et al*. (2018) pointed out that when shale transforms from completely plastic state to absolutely brittle state, its brittleness index increases from 0 to 1 correspondingly. Meanwhile, there is no specific method to classify the brittle degree of rock qualitatively, which needs further discussion. And the determination of existing brittleness index mostly relies on static or quasi-static tests, while coal rock still exhibits brittle-ductile transition characteristics under the action of confining pressure and dynamic strain rate. Therefore, it is significant to determine coal rock brittleness index in dynamic test and study the influence of confining pressure and strain rate on it.

In order to provide a reasonable basis for safe and efficient coal mining during dynamic excavation process, dynamic impact compression tests of Furong Baijiao coal rock under four confining pressures (0, 4, 8 and 12 MPa) and different strain rates (40-270 s^{-1}) were carried out by split Hopkinson pressure bar (i.e., SHPB) of School of Resources and Safety Engineering of Central South University. After that, its dynamic mechanical properties, deformation and failure characteristics, and brittleness traits were studied in this research.

2. Tests and methods

2.1 Test equipment and specimen preparation

Fig. 1 shows SHPB test device with confining pressure. Elastic bars of the test system were made of 40Cr alloy steels with a diameter of 50 mm, a length of 2 m, a density of 7697 kg/m^3, a Poisson's ratio of 0.28, and a longitudinal wave velocity of 5410 m/s. The test system is controlled by impact pressure, and strain rate is obtained by different pressure. Before testing, Vaseline is uniformly coated on the contact surface of specimen and incident/transmitted bar to reduce friction effect. When loading, first a spindle-shaped striker was used in this test system to generate a stable half-sine incident stress wave, which can eliminate lateral oscillation and reduce dispersion effect. Then the pulse signals are collected by strain gages on elastic bars, which are transmitted to CS-1D super-dynamic strain gauge later. Finally, the incident, reflection and transmission strain values are shown by DL750 oscilloscope.

Coal rock for this research was taken from the 2# coal seam of Furong Baijiao Coal Mine in Yibin, Sichuan, China, with a buried depth of +350 m. The coal rock is anthracite coal rich in ash and sulfur, mainly composed of 79.02% amorphous minerals, 10.07% quartz, 5.88% calcite and 4.85% kaolinite. According to recommended standards of the International Society of Rock Mechanics and Rock Engineering (Ulusay 2015), coal rock was processed into Φ50 mm×L50 mm cylindrical specimens (the ratio of length to diameter of 1:1). Surface planeness of specimen is controlled to ±0.05 mm, and the vertical deviation of the upper and lower surfaces is ±0.25°. In the test, thirty-two coal rock samples were prepared, and eight samples were used under each confining pressure.

2.2 Test validity verification

Figs. 2 and 3 are the stress wave waveform and stress balance analysis diagram of representative coal rock respectively. As can be seen from Fig. 2, there is no obvious transverse vibration of stress waves under uniaxial and triaxial conditions, indicating that the one-dimensional propagation assumption can be well realized in process of

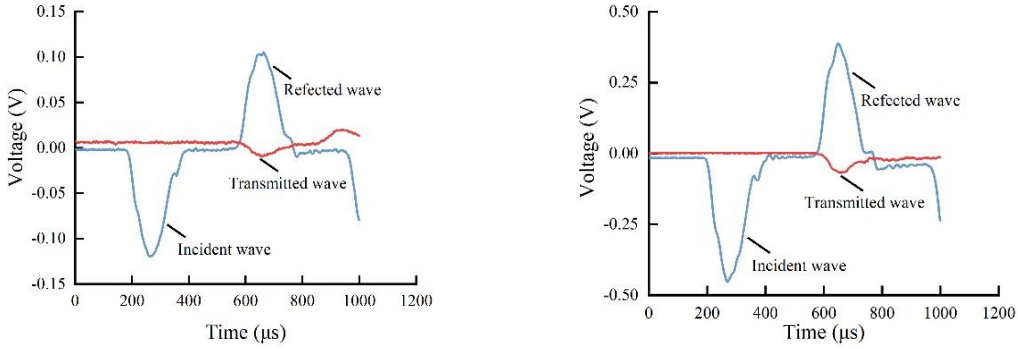

(a) Uniaxial state (b) Triaxial state

Fig. 2 Dynamic impact test waveform of representative coal rock

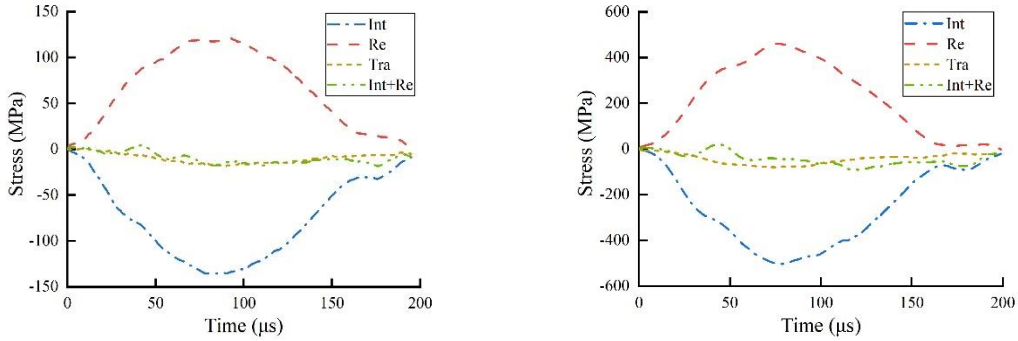

(a) Uniaxial state (b) Triaxial state

Fig. 3 Stress balance analysis in dynamic impact compression test of coal rock

stress wave propagation. From Fig. 3, it can be seen that during dynamic loading, the sum of incident stress and reflection stress (Int+Re) is basically consistent with transmitted stress (Tra), which indicates that the stress on both ends of coal rock specimen matches and the sample is in stress equilibrium state.

2.3 Test principle

Based on the assumption of stress wave one-dimensional propagation and stress uniformity, the relationship among stress, strain, and strain rate of coal rock obtained by the two-wave method is as follows

$$\begin{cases} \sigma(t) = \dfrac{A_0 E_0}{A_s} \varepsilon_t(t) \\ \dot{\varepsilon}(t) = -\dfrac{2C_0}{L_s} \varepsilon_r(t) \\ \varepsilon(t) = \int_0^t \dot{\varepsilon}(t)\mathrm{d}t = -\dfrac{2C_0}{L_s} \int_0^t \varepsilon_r(t)\mathrm{d}t \end{cases} \tag{1}$$

Where A_0, E_0 and C_0 are cross-sectional area, elastic modulus and wave velocity of elastic bar respectively; A_s and L_s are specimen's cross-sectional area and length; $\varepsilon_r(t)$ and $\varepsilon_t(t)$ are reflection and transmission strains in the bar; And t is the impact time.

During SHPB dynamic impact test, the total dissipated energy W_d absorbed by coal rock can be described by

$$W_d = W_i - W_r - W_t \tag{2}$$

$$W = \frac{A_0}{\rho_0 C_0} \int_0^t \sigma^2(t)\mathrm{d}t \tag{3}$$

Where W_i, W_r and W_t are incident energy, reflection energy and transmission energy respectively, which can be calculated by Eq. (3); And ρ_0 is the density of elastic bar.

Meanwhile, the dissipated energy density ω_d can be described by

$$\omega_d = \frac{W_d}{V} \tag{4}$$

Where V is the volume of coal rock sample.

3. Test results and analysis

3.1 Dynamic stress-strain curve

As shown in Fig. 4, four stress-strain curves of representative coal rock are selected for analysis under each of the four confining pressures. As can be seen from the figure, there is no obvious difference between the compaction stage and linear elastic stage due to the short and strong impact. Thus, the dynamic stress-strain curve of coal rock sample can be divided into linear elastic stage, plastic yield stage and post-peak softening stage. In linear elastic stage, the internal cracks of coal rock maintain stable after they closed and converged. In plastic yield stage, originate fissures rapidly expanded and new crack were generated, then coal rock specimen entered a longer period

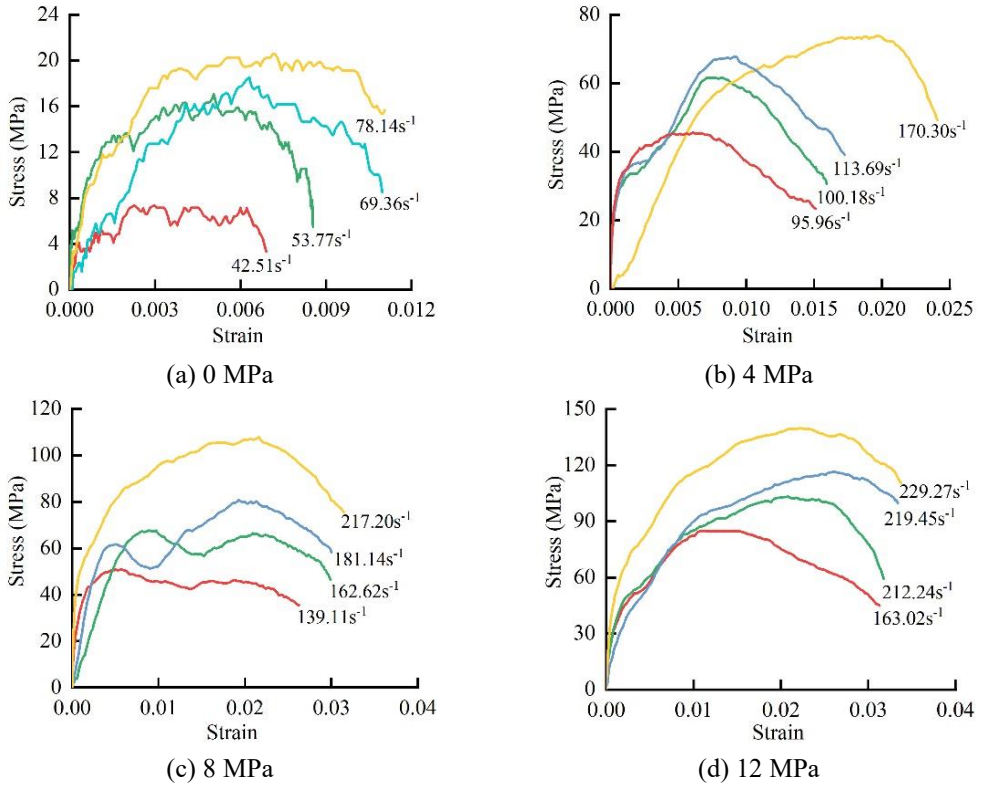

(a) 0 MPa (b) 4 MPa

(c) 8 MPa (d) 12 MPa

Fig. 4 Dynamic stress-strain curve of representative coal rock

Table 1 Basic parameters of coal rock samples

σ_3/MPa	$\dot{\varepsilon}$ /s^{-1}	σ_d/MPa	ε_d	σ_3MPa	$\dot{\varepsilon}$ /s^{-1}	σ_d/MPa	ε_d
0	42.51	7.53	0.0030	8	137.74	64.93	0.0087
	53.77	17.09	0.0051		139.11	50.87	0.0063
	60.61	20.33	0.0065		162.62	67.61	0.0091
	69.36	18.49	0.0063		167.64	55.50	0.0157
	71.90	20.99	0.0042		181.82	80.89	0.0193
	76.09	23.29	0.0075		189.35	55.00	0.0082
	78.14	21.05	0.0072		210.11	77.01	0.0106
	87.59	18.54	0.0093		217.20	107.88	0.0216
4	95.96	46.05	0.0060	12	163.02	84.90	0.0108
	98.48	36.50	0.0074		206.64	102.34	0.0186
	100.18	61.67	0.0083		212.24	103.26	0.0202
	113.69	68.72	0.0092		219.45	116.55	0.0255
	134.55	67.50	0.0089		228.10	79.97	0.0176
	148.43	43.18	0.0122		229.27	139.67	0.0225
	163.52	51.60	0.0090		244.18	128.70	0.0201
	170.30	73.80	0.0199		261.34	114.70	0.0287

of plastic deformation. After peak stress, stress-strain curve drops, and strain softening occurs, which indicating that the bearing capacity of coal rock samples decreases.

It can be seen clearly that the stress-strain curve under triaxial state is smoother than that of uniaxial state, which is due to the influence of confining pressure on coal rock fractures. Under the same confining pressure, initial elastic modulus of coal rock increases with strain rate increasing. And the proportion of linear elastic stage in whole failure process decreases, while the proportion of plastic yield stage increases. This is because increasing strain rate makes energy obtained in initial stage increase and crack closure gets faster, thereby linear elastic stage shortens. When the strain rates are similar, as confining pressure increases, peak stress significantly increases, the plastic deformation gradually occupied the dominant position, and the drop speed of post-peak stress slowed down relatively.

3.2 Dynamic mechanical characteristics

Average strain rate ε, dynamic compressive strength σ_d and peak strain ε_d of coal rock samples are calculated according to Eq. (1). And the results are listed in Table 1. It can be seen from Table 1 that the dynamic compressive strength and peak strain of coal rock samples are somewhat discrete with the increase of strain rate in the same state, but they show an increasing trend on the whole. As confining pressure varies from 0 to 12 MPa, compressive strength rises from about 20 MPa to more than 120 MPa, and peak strain change from less than 0.01 to over 0.02. The growth in compressive strength and axial deformation respectively indicates that coal rock stiffness and plastic deformation enhance. In the range of 0-4 MPa, the confining pressure effect of compressive strength is the most obvious, and the maximum increase is close to 10 times. Therefore, confining pressure can improve the compressive strength and enhance plastic deformation of coal rock.

3.3 Dynamic failure characteristics

Fig. 5 shows the failure characteristics of representative coal rock under different confining pressures. Dynamic impact compression failure patterns of coal rock are distinct under different loading conditions. From Fig. 5(a), it can be

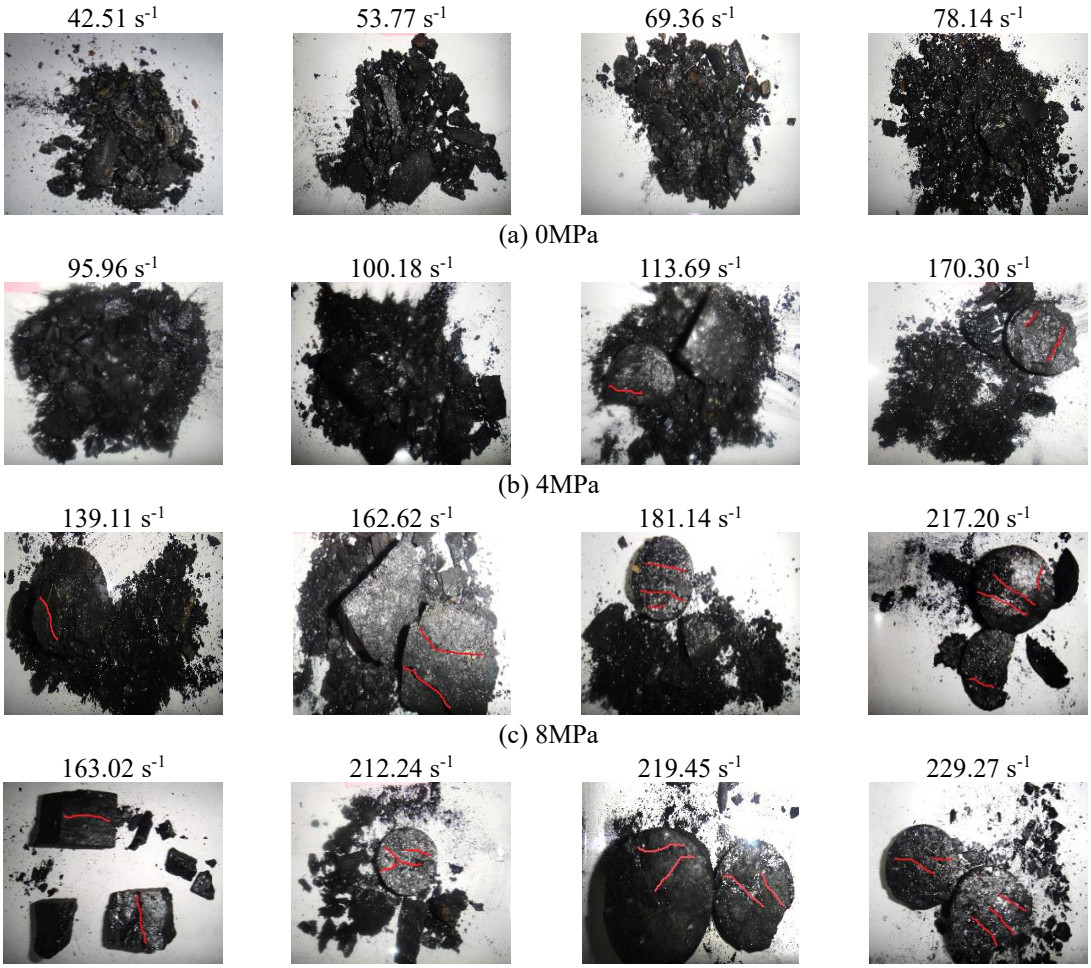

Fig. 5 Dynamic failure characteristics of representative coal rock

seen that coal rock specimen in uniaxial state appeared axial splitting failure due to tensile stress and produced fragments of different sizes, showing obvious brittleness characteristics. With strain rate increasing, the destruction of coal rock became more severe, and more small particle fragments were formed. Due to the higher strain rate, the impact loading time is not enough to complete crack propagation, so stress level rises sharply to causing rock break more severe. At this time, more energy is needed and the increase in energy is realized by the increase in stress, which means that high strain rate makes coal rock strength and failure degree improve.

In triaxial state, coal rock samples are mainly subjected to compression-shear failure under the action of shear stress, forming large fragments with microcracks on the surface and accompanying surrounding shedding, and plastic characteristics are enhanced. Comparing Figs. 5(b)-(d), the conclusion can be got that the growth in confining pressure adds to the possibility of coal rock crushing into large fragments. In particular, coal rock samples under 12 MPa confining pressure with strain rates of 219.45 s^{-1} and 229.27 s^{-1} ruptured into two nearly complete blocks after impact compression, this is because that confining pressure restricts the crack propagation and lateral deformation in coal and rock. Under the same confining pressure, with the increase of strain rate, large fragments and cracks on the surface of broken blocks increase (as can be seen from the red line in Fig. 5). To sum up, confining pressure can effectively control the broken degree of coal rock under dynamic impact compression, and as confining pressure improves, coal rock shows obvious brittle-plastic transition, and its failure mode changes from axial splitting failure to compression-shear failure.

3.4 Average fragmentation and fractal dimension

Because coal rock specimens under uniaxial and triaxial impact compression were fractured into many fragmentations of various sizes. Thus, these fragments were screened respectively by standard sieves of 0.25 mm, 0.5 mm, 1.0 mm, 5.0 mm, 10.0 mm, 20.0 mm, 40.0 mm and 50.0 mm, the sieving diagrams of representative coal rock samples are shown in Table 2. After sieving, the weighted average value of each particle size content is taken as the average fragmentation d_m to describe the fragmentation degree of coal rock, the calculation formula of d_m is

$$d_m = \frac{\Sigma\left(r_i d_i\right)}{\Sigma r_i} \tag{5}$$

Table 2 Fracture characteristics analysis of representative coal rock under different confining pressures

Sample	Particle sieving analysis			Sieving curve		d_m/mm	D_b	R^2
	r/mm	$M(r)$/g	r_i/%	ln$r$	ln[$M(r)/M$]			
σ_3=0MPa; $\dot{\varepsilon}$=69.36s^{-1} 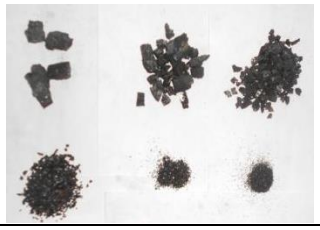	50	104	100.00	3.91	4.61	32.31	2.103	0.983
	40	104	100.00	3.69	4.61			
	20	78.5	75.48	3.00	4.32			
	10	44.5	42.79	2.30	3.76			
	5	18	17.31	1.61	2.85			
	1	4	3.85	0.00	1.35			
	0.5	2	1.92	-0.69	0.65			
	0.25	0	0.00	-1.39				
σ_3=4MPa; $\dot{\varepsilon}$=113.69s^{-1} 	50	132	100.00	3.91	4.61	31.97	2.306	0.990
	40	132	100.00	3.69	4.61			
	20	68	51.52	3.00	3.94			
	10	54.5	41.29	2.30	3.72			
	5	34	25.76	1.61	3.25			
	1	11	8.33	0.00	2.12			
	0.5	5.5	4.17	-0.69	1.43			
	0.25	0	0	-1.39				
σ_3=8MPa; $\dot{\varepsilon}$=217.20s^{-1} 	50	131.5	100.00	3.91	4.61	39.92	1.795	0.984
	40	56	42.59	3.69	3.75			
	20	36.5	27.76	3.00	3.32			
	10	13	9.89	2.30	2.29			
	5	5	3.80	1.61	1.34			
	1	1	0.76	0.00	-0.27			
	0.5	0	0.00	-0.69				
	0.25	0	0.00	-1.39				
σ_3=12MPa; $\dot{\varepsilon}$=212.24s^{-1} 	50	129.5	100.00	3.91	4.61	36.90	2.201	0.983
	40	73.5	56.76	3.69	4.04			
	20	35.5	27.41	3.00	3.31			
	10	25	19.31	2.30	2.96			
	5	12.5	9.65	1.61	2.27			
	1	4.5	3.47	0.00	1.25			
	0.5	2.5	1.93	-0.69	0.66			
	0.25	0	0.00	-1.39				

Where d_i is the size of each particle grade; r_i is the cumulative mass percentage of coal rock in each particle grade.

Since coal rock fragment have obvious statistical self-similarity, fractal theory can be better used to discussion. In this paper, using mass-size relation to calculate the fractal dimension D_b

$$\begin{cases} D_b = 3-\alpha \\ \alpha = \dfrac{\ln\left[M(r)/M\right]}{\ln r} \end{cases} \tag{6}$$

Where $M(r)$ is the cumulative mass of block with diameter smaller than r; M is the mass of coal rock specimen; α is the mass-size distribution index, take ln[$M(r)/M$] as ordinate and ln$r$ as abscissa to draw a curve and conduct linear fitting, and slope of the straight line is α. The calculation results of dm and D_b are shown in Table 2.

Fig. 6 shows the variation of average fragmentation and fractal dimension with strain rate under different confining pressures. As can be seen from the figure, average fragmentation of coal rock under uniaxial state is concentrated in the range from 30 mm to 35 mm, which generally shows a downward trend with strain rate increasing. This is because high strain rate usually causes internal cracks of coal rock to propagate and extend rapidly, and its broken process becomes more thorough resulting in

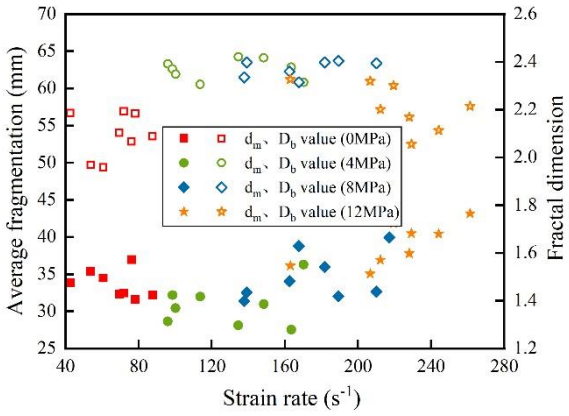

Fig. 6 Relationship between average fragmentation, fractal dimension and strain rate

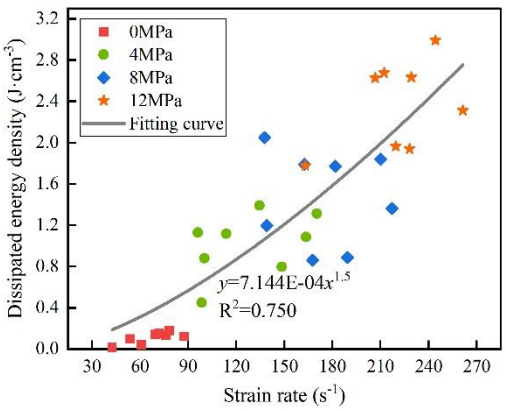

Fig. 7 Dissipated energy density of coal rock under different strain rates

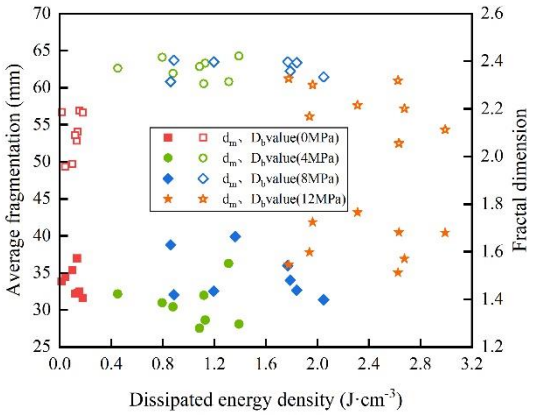

Fig. 8 Relationship between average fragmentation, fractal dimension and dissipated energy density

more fragments, which can also be seen in Fig. 5(a). Under triaxial condition, average fragmentation is larger than that in uniaxial state except for 4 MPa confining pressure. When confining pressure rises from 4 MPa to 8 MPa and then to 12 MPa, average fragmentation increases from about 30 mm to 35 mm and then to 40mm. As mentioned in section 3.3, confining pressure restrains the crack propagation and evolution of coal rock, and the increase of confining pressure leads to the smaller stress difference between two directions of coal rock sample, so the fragments get larger. However, under the same confining pressure, the variation law of average fragmentation of coal rock with strain rate is not obvious.

It can also be seen from Fig. 6 that fractal dimension of coal rock under dynamic impact compression is concentrated in the range from 2.1 to 2.4, indicating that the mass of small-scale fragments is relatively large. In uniaxial state, fractal dimension increases from 2.0 to about 2.2 as strain rate increases. However, under triaxial condition, when confining pressure changes from 4 MPa to 12 MPa, fractal dimension with the increase of strain rate first increases slightly and then decreases obviously and then tends to be stable. Since the fractal dimension stabilizes around 2.1 as confining pressure increases to 12 MPa, it can be seen that improving confining pressure continuously cannot result in more fractured coal rock fragmentation. From the relationship between average fragmentation and fractal dimension can be known that the larger the fractal dimension is, the more brittle coal rock is, and the smaller the fragments are. Since the fracture degree of coal rock under 4 MPa confining pressure and 100-140 s^{-1} strain rate is high, the corresponding average fragmentation is less than 30 mm, controlling the lower confining pressure and higher strain rate can improve the efficiency of coal rock mining.

3.5 Energy dissipation law of coal rock failure

Rock failure is a process from energy accumulation to energy dissipation and finally to energy release, and the scale of rock fragments after failure is closely related to the amount of energy dissipated. The dissipated energy density of each coal rock sample is calculated according to Eqs. (2)-(4), and its variation law is shown in Fig. 7. As can be seen from the figure that the dissipated energy density of coal rock under different confining pressures generally increases in a power function with the increase of strain rate. Under uniaxial condition, the maximum dissipated energy density of coal rock is less than 0.2 $J \cdot cm^{-3}$, and the growth rate of dissipated energy density is not obvious with strain rate increasing. Under triaxial state, coal rock dissipated energy density is much higher than that in uniaxial state, and its maximum value is 3.0 $J \cdot cm^{-3}$, almost fourteen times than that of uniaxial state, which indicate that the effect of confining pressure on energy dissipation in the process of dynamic impact failure is significant. While under the same confining pressure, dissipation energy density is concentrated in a certain range, and the variation law with strain rate is not obvious.

Fig. 8 shows the variation of average fragmentation and fractal dimension of coal rock with the dissipation energy density. It can be found that the distribution law of Fig. 8 and Fig. 6 are relatively similar, showing that energy is the essence of failure, and the failure degree of coal rock can also be judged by energy. Under low confining pressure conditions (such as 0 MPa and 4 MPa), the more energy dissipated per unit volume of coal rock sample, the larger fractal dimension and the smaller fragmentation. This is because the more energy coal rock specimen absorbs, the faster crack propagates and the more intense coal rock breaks. As confining pressure becomes higher (such as 8, 12 MPa), the average fragmentation is stable at 35-40 mm, and the fractal dimension is smaller than that of low confining pressure. The results show that infinitely increasing dissipated energy density of coal rock specimen cannot make average fragmentation and fractal dimension change greatly, which also indirectly reflects that confining pressure can effectively control the failure degree of coal rock.

4. Brittleness identification based on the maximum damage rate

The impactive instability occurring in coal mining is a typical brittle failure process, usually accompanied by the

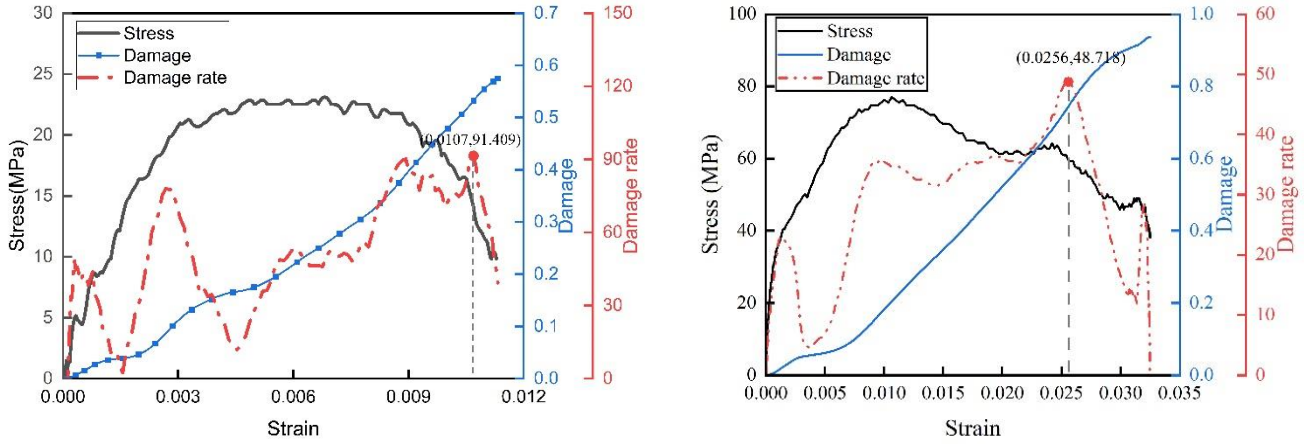

(a) Uniaxial state (b) Triaxial state

Fig. 9 Stress-strain, damage evolution and damage rate curve of representative coal rock

release of a large amount of energy, causing coal rock burst to form many fragments of different sizes. In order to promote coal rock failure or control its break degree, the brittleness index can be defined to evaluate and describe the brittleness degree of coal rock.

4.1 Definition of brittleness index

There are many definition methods of rock brittleness index, such as the strength, Poisson's ratio, elastic modulus and stress-strain curve. However, coal rock as a kind of rock with primary joints and highly developed fissures, its stress-strain curve obtained under dynamic impact compression is not smooth, especially the stress-strain curves at 0 MPa fluctuate greatly. Meanwhile, the determination of elastic modulus is subjective and residual strength is not obvious, so there are some limitations in using existing methods to determine the brittleness index of coal rock. Coal rock failure is a gradual damage process, and damage is essentially a process of releasing accumulated elastic energy. It can be seen from Fig. 9 that damage evolution curve is the result of damage variable accumulation. Damage variable represent the failure degree after coal rock impact compression, but it cannot reflect the release rate of accumulated elastic energy in coal rock, which can be indirectly reflected by damage rate. Since the maximum damage rate is a measure of the maximum failure severity of coal rock, and it is also the starting point for dynamic damage (Cai *et al*. 2011). Hu *et al*. (2020) established a brittleness index B_D to describe coal rock brittleness degree based on the maximum damage rate, the calculation method is shown in Eq. (7). In this paper, the maximum damage rate is obtained by deriving damage variable, and damage variable is the ratio of dissipation energy density to total absorption energy density.

$$B_D = \frac{\dot{D}_{\max}}{\varepsilon_m \times 10^3} \tag{7}$$

Where ε_m is corresponding strain value of the maximum damage rate. Then damage D and the maximum damage rate $\dot{D}_{\max}$ can be calculated by

$$\begin{cases} D = \dfrac{\omega_d}{u} \\ \dot{D}_{\max} = \left(\dfrac{\mathrm{d}D}{\mathrm{d}\varepsilon}\right)_{\max} \end{cases} \tag{8}$$

Where u is the total absorbed energy density, which is the area enclosed by the stress-strain curve in dynamic test

$$u = \int \sigma d\varepsilon \tag{9}$$

Fig. 9 is the stress-strain curve, damage evolution curve and damage rate curve of coal rock sample under uniaxial and triaxial state respectively. It can be obtained from Fig. 9 that damage rate curves under uniaxial and triaxial state have some differences in each stage, but damage rate shows a trend of increasing first to the maximum damage rate and then rapidly decreasing on the whole. Due to internal fractures propagation, rock damage is not a continuous process, so damage rate curve will fluctuate before the maximum damage rate appears. Comparing with Figs. 9(a) and (b), it can be found that the fluctuation of damage rate curve in triaxial state is smaller than that in uniaxial state, this is because confining pressure weakens the influence of internal fissures development on the damage process of coal rock. In both two states, the maximum damage rate point of coal rock usually occurs in post-peak stage of stress-strain curve, indicating that the severity of coal rock failure reached the maximum after the peak stress. Since the macroscopic failure of coal rock samples usually occurs after peak stress, and the post-peak mechanical behavior of rock can better represent its brittleness. Therefore, it is meaningful to determine brittleness index of coal rock through the maximum damage rate.

4.2 Brittleness characteristics of coal rock

The maximum damage rate of each coal rock sample is calculated according to Eq. (8), and then bring the maximum damage rate and its corresponding strain value into Eq. (7) to calculate the brittleness index. Calculation results are listed in Table 3. It can be seen from the table that as the confining pressure changes from 0 MPa to 12

Table 3 Calculation of coal rock brittleness index under different confining pressure

σ_3/MPa	$\dot{\varepsilon}$ /s^{-1}	$\dot{D}_{max}$	ε_m	B_D	σ_3/MPa	$\dot{\varepsilon}$ /s^{-1}	$\dot{D}_{max}$	ε_m	B_D
0	42.51	121.508	0.0078	15.658	8	137.74	60.448	0.0121	4.981
	53.77	163.453	0.0077	21.275		139.11	46.495	0.0105	4.435
	60.61	147.578	0.0010	14.769		162.62	52.223	0.0187	2.787
	69.36	216.480	0.0116	18.662		167.64	60.570	0.0306	1.979
	71.90	72.772	0.0037	19.854		181.82	51.641	0.0212	2.441
	76.09	91.409	0.0107	8.5429		189.35	53.232	0.0167	3.185
	78.14	148.369	0.0133	11.156		210.11	48.718	0.0256	1.904
	87.59	140.823	0.0120	11.787		217.20	30.210	0.0286	1.057
4	95.96	128.055	0.0106	12.037	12	163.02	42.169	0.0269	1.568
	98.48	59.757	0.0076	7.862		206.64	33.895	0.0321	1.058
	100.18	103.077	0.0110	9.366		212.24	54.135	0.0286	1.891
	113.69	83.800	0.0181	4.635		219.45	32.010	0.0333	0.961
	134.55	52.362	0.0169	3.091		228.10	47.040	0.0332	1.415
	148.43	72.616	0.0161	4.511		229.27	30.606	0.0309	0.991
	163.52	86.499	0.0088	9.873		244.18	33.230	0.0300	1.107
	170.30	72.709	0.0206	3.534		261.34	35.231	0.0316	1.116

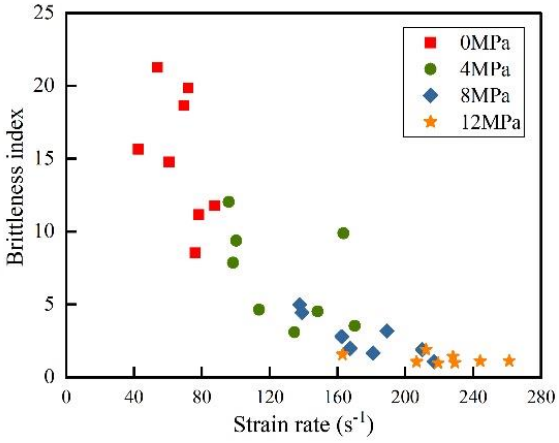

Fig. 10 Relationship between confining pressure and brittleness index of coal rock

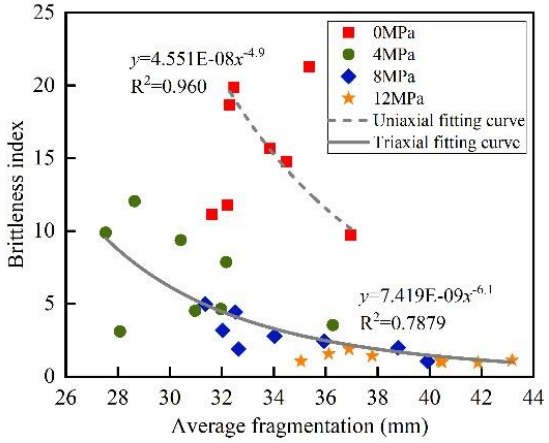

Fig. 11 Relationship between average fragmentation and brittleness index of coal rock

MPa, the maximum damage rate of coal rock decreases from over 100 to near 30, and the strain corresponding to the maximum damage rate increases. It shows that the damage severity of coal rock gradually reduces as confining pressure increases, while it does not change significantly with strain rate.

The variation of brittleness index with strain rate under different confining pressure is shown in Fig. 10. From the figure, it can be seen that the brittleness indexes B_D of coal rock are mainly concentrated in the range from 1 to 20. The B_D value declined as strain rate increases under different confining pressure, and its reduction decreases with the increase of confining pressure. When confining pressure reaches to 12 MPa the B_D value tends to be stable, which shows that the strain rate effect of brittleness index weakens with increasing confining pressure. Brittleness index can measure the brittleness degree of rock, the higher B_D value is, the more brittle rock is. Since brittleness index decreases as confining pressure increases, which indicating that the brittleness of coal rock gradually weakens as confining pressure rises. Therefore, brittleness index can well reflect the brittle-plastic transition characteristics of coal rock. How to use the brittleness index to define brittle plasticity of coal rock will be discussed in the next section.

Rock brittleness is an important attribute for fragility evaluation, the stronger the rock brittleness, the more easily it will burst into small fragments, reversely it forms large pieces if the brittleness is weak. Fig. 11 shows the relationship between the average fragmentation and brittleness index of coal rock under different confining pressures. It can be obtained from the diagram that the brittleness index of coal rock decreases as a power function with the increase of average fragmentation under both uniaxial and triaxial conditions, and the relationship between them can be described by Eq. (10). In order to show the variation law of brittleness index with average fragmentation clearly, three discrete points were removed when fitting the test data in uniaxial condition. Meanwhile, as can be seen in the figure that when brittleness index is between 10 and 15, the average fragmentation in 4 MPa is less than that in 0 MPa. It indicates coal rock is more completely broken in 4 MPa when there is not much different in brittleness, which is consistent with the results obtained in Section 3.4. That is, under the effect of lower

Table 4 The brittleness classification

Degree of brittleness	The range of B_D value
high brittleness	9.0~22.0
moderate brittleness	4.0~9.0
low brittleness	1.5~4.0
weak brittleness	0~1.5

confining pressure and medium strain rate, the more severe the damage of coal rock, the smaller the fragments formed. In summary, average fragmentation is closely related to brittleness index, coal rock brittleness can be evaluated from the perspective of macroscopic damage by average fragmentation.

$$\begin{cases} B_D = 4.551E\text{-}08 d_m^{-4.9}, \sigma_3 = 0 \\ B_D = 7.419E\text{-}09 d_m^{-6.1}, \sigma_3 \neq 0 \end{cases} \quad (10)$$

5. Discussion and prospect

5.1 Discussion

In this paper, based on the dynamic stress-strain curve and failure characteristics of coal rock, the brittleness degree of coal rock under dynamic impact compression can be defined and divided into four grades according to B_D value: (1) In low confining pressure, the stress-strain curve of coal rock has a large stress drop, whose residual strength is close to 0 and plastic deformation is small. Some coal rock samples under 0 MPa and 4 MPa confining pressure mainly break into many small particles by the action of tensile stress, and the corresponding B_D value is between 9.0 and 22.0. Therefore, when $9.0<B_D<22.0$, the brittleness is high. (2) As confining pressure increases, the plastic deformation of some coal rock in 4 MPa and 8 MPa enhances, and large-scale fragments begin to appear under the coaction of tensile stress and shear stress. The corresponding B_D value is between 4.0 and 9.0, so the brittleness is moderate when $4.0<B_D<9.0$. (3) When the confining pressure is higher, the stress drop decreases and the plastic deformation further increases. The coal rock samples in 8 MPa and few in 12 MPa mainly undergo shear failure by the action of shear stress, and the corresponding B_D value is between 1.5 and 4.0. Therefore, when $1.5<B_D<4.0$, the brittleness is low. (4) As confining pressure reaches 12MPa, the stress drop is relatively small, and coal rock samples are mostly sheared into two large blocks. The corresponding B_D value is between 0 and 1.5 in the state, thence the brittleness is weak when $0<B_D<1.5$. The brittleness classification results of coal rock under dynamic impact are summarized in Table 4. Since the fluctuation of strain rate does not affect the decreasing trend of brittleness index with increasing confining pressure that can be seen in Fig. 3, the brittleness degree of coal rock can be directly determined by B_D value.

5.2 Prospect

Impact instability and rock burst disaster that always occur in mining and underground engineering excavation are typical brittle failure process. In order to predict and reduce the occurrence of such disasters, brittleness index can be used to evaluate the impact and burst proneness of rock (Afraei *et al*. 2018). At present, many scholars have proposed the brittle index criterion of impact and burst proneness. For instance, Wang and Park (2001) took the ratio of uniaxial compressive strength and tensile strength as the brittleness index of granite, and classified its burst grades according to brittleness index. In this paper, the brittleness index B_D is established based on the maximum damage rate. Cai *et al*. (2011) once pointed out that the maximum damage rate can be used as an evaluation index of coal rock impact proneness. The greater the maximum damage rate, the more thorough the destruction of coal rock, and the stronger its impact proneness. Thence, could the brittleness index established in this paper also be used to evaluate the impact proneness of coal rock? This deserves in-depth consideration in future research.

6. Conclusions

In this paper, the split Hopkinson pressure bar is used to conduct dynamic impact compression tests on coal rock under four confining pressures (0, 4, 8 and 12 MPa) and different strain rates (40-270 s^{-1}).

- Dynamic stress-strain curves of coal rock can be divided into linear elastic stage, plastic yield stage and post-peak softening stage. With increasing strain rate, compressive strength and peak strain show a growing trend. As confining pressure rises from 0 MPa to 12 MPa, compressive strength raises more than 6 times and peak strain increase significantly. Meanwhile plastic deformation of coal rock enhances, and its failure mode changes from splitting failure to compression-shear failure, showing obvious brittle-plastic transition characteristics.
- The dissipated energy density of coal rock rises from less than 0.2 $J \cdot cm^{-3}$ to about 3.0 $J \cdot cm^{-3}$ as confining pressure increases from 0 MPa to 12 MPa, while it does not change obviously with the strain rate under the same confining pressure. The greater the dissipated energy density, the smaller the coal rock fragment and the larger the fractal dimension. However, there are always large-scale fragments even if the dissipation energy is very large, which is because confining pressure restrains the internal cracks development of coal rock. Therefore, the failure degree of coal rock tends to be stable as confining pressure reaches 12 MPa, the corresponding average fragmentation and fractal dimension are respectively maintained at about 40 mm and 2.2.
- In order to describe coal rock brittleness, the derivative of damage variable to strain is defined as the maximum damage rate. Under uniaxial and triaxial conditions, the maximum damage rate of coal rock usually occurs in post-peak stage, which indicates that its macroscopic failure always occurs in this stage. With the increase of confining pressure, the maximum damage rate decreases from more than 100 to about 30, showing the damage degree of coal rock weakens severely.

• The ratio of the maximum damage rate to its corresponding strain is taken as brittleness index. B_D value gradually declines with increasing confining pressure, and its decreasing amplitude gradually reduces as strain rate increases. When confining pressure reaches 12 MPa, B_D value stabilizes at 1 even though the strain rate is relatively large. According to the B_D value, coal rock brittleness can be divided into four grades: when $9.0<B_D<22.0$, it is high; when $4.0<B_D<9.0$, it is moderate; when $1.5<B_D<4.0$, it is low; and when $0<B_D<1.5$, it is weak.

Acknowledgments

This research was funded by the General project of Sichuan Natural Science Foundation (Grant No: 2022NSFSC0279, 2022NSFSC1009), the Key Scientific Research Fund of Xihua University (Grant No: Z17113), and Graduate Innovation Fund of Xihua University (Grant No: YCJJ2021056).

References

Afraei, S., Shahriar, K. and Madani, S.H. (2018), "Statistical assessment of rock burst potential and contributions of considered predictor variables in the task", *Tunn. Undergr. Space Technol.*, **72**, 250-271. https://doi.org/10.1016/j.tust.2017.10.009.

Al-Salloum, Y., Alsayed, S., Almusallam, T., Ibrahim, S.M. and Abbas, H. (2014), "Investigations on the influence of radial confinement in the impact response of concrete", *Comput. Concrete*, **14**(6), 675-694. https://doi.org/10.12989/cac.2014.14.6.675.

Bernabe, Y. and Revil, A. (1995), "Pore-scale heterogeneity, energy dissipation and the transport properties of rocks", *Geophys. Res. Lett.*, **22**(12), 1529-1532. https://doi.org/10.1016/0148-9062(96)85059-5.

Cai, W., Dou, L.M., Han, R.J., Zhang, G.H., and Li, X.W. (2011), "Bursting liability of coal based on damage statistical constitutive model", *J. China Coal Soc.*, **36**(S2), 346-352. https://doi.org/10.13225/j.cnki.jccs.2011.s2.029.

Demirdag, S., Tufekci, K., Kayacan, R., Yavuz, H. and Altindag, R. (2010), "Dynamic mechanical behavior of some carbonate rocks", *Int. J. Rock Mech. Min. Sci*., **47**(2), 307-312. https://doi.org/10.1016/j.ijrmms.2009.12.003.

Feng, J.J., Wang, E.Y., Shen, R.X., Chen, L., Li, X.L. and Xu, Z.Y. (2016), "Investigation on energy dissipation and its mechanism of coal under dynamic loads", *Geomech. Eng.*, **11**(5), 657-670. https://doi.org/10.12989/gae.2016.11.5.657.

Ghadernejad, S., Nejati, H.R. and Yagiz, S. (2020), "A new rock brittleness index on the basis of punch penetration test data", *Geomech. Eng.*, **21**(4), 391-399. https://doi.org/10.12989/gae.2020.21.4.391.

Gong, F.Q., Si, X.F., Li, X.B. and Wang, S.Y. (2019), "Dynamic triaxial compression tests on sandstone at high strain rates and low confining pressures with split Hopkinson pressure bar", *Int. J. Rock Mech. Min. Sci.*, **113**, 211-219. https://doi.org/10.1016/j.ijrmms.2018.12.005.

Hu, Q.B., Liang, H.A., Yang, T., Cheng, X.J., Chen, H.K. and Zhang, L.P. (2020), "A new method for rock brittleness evaluation based on statistical damage constitutive relation", *J Harbin Inst. Technol.*, **52**(11), 147-156. https://doi.org/10.11918/201906094.

Hucka, V. and Das, B. (1974), "Brittleness determination of rocks by different methods", *Int. J. Rock Mech. Min. Sci.*, **11**(10), 389-392. https://doi.org/10.1016/0148-9062(74)91109-7.

Kim, E.H., Garcia, A. and Changani, H. (2018), "Fragmentation and energy absorption characteristics of Red, Berea and Buff sandstones based on different loading rates and water contents", *Geomech. Eng.*, **14**(2), 151-159. https://doi.org/10.12989/gae.2018.14.2.151.

Kivi, R.I., Ameri, M. and Molladavoodi, H. (2018), "Shale brittleness evaluation based on energy balance analysis of stress-strain curves", *J. Pet. Sci. Eng*., **167**, 1-19. https://doi.org/10.1016/j.petrol.2018.03.061.

Liu, X.H., Dai, F., Zhang, R. and Liu, J.F. (2015), "Static and dynamic uniaxial compression tests on coal rock considering the bedding directivity", *Environ. Earth Sci*., **73**(10), 5933-5949. https://doi.org/10.1007/s12665-015-4106-3.

Lu, Y.Q., Liu, X.H., Xie, J., He, Z.Q. and Li, C. (2019), "The energy evolution characteristics of coal under different dynamic strain rates and confining pressures", *Therm. Sci*., **23**(3), 1409-1416. https://doi.org/10.2298/tsci1808102051.

Meng, F.Z., Zhou, H., Zhang, C.Q., Xu, R.C. and Lu, J.J. (2015), "Evaluation methodology of brittleness of rock based on post-peak stress–strain curves", *Rock Mech. Rock Eng*., **48**(5), 1787-1805. https://doi.org/10.1007/s00603-014-0694-6.

Moska, R., Kasza, P. and Maslowski, M. (2018), "Rock anisotropy and brittleness from laboratory ultrasonic measurements in the service of hydraulic fracturing", *Acta Geodyn. Geomater.*, **15**(1), 67-76. https://doi.org/10.13168/AGG.2018.0005.

Munoz, H., Taheri, A. and Chanda, E.K. (2016), "Fracture energy-based brittleness index development and brittleness quantification by pre-peak strength parameters in rock uniaxial compression", *Rock Mech. Rock Eng.*, **49**(12), 4587-4606. https://doi.org/10.1007/s00603-016-1071-4.

Omidvar, M., Iskander, M. and Bless, S. (2012), "Stress-strain behavior of sand at high strain rates", *Int. J. Impact Eng.*, **49**, 192-213. https://doi.org/10.1016/j.ijimpeng.2012.03.004.

Özfırat, M. K., Yenice, H., Şimşir, F. and Yaralı, O. (2016), "A new approach to rock brittleness and its usability at prediction of drillability". *J. Afr. Earth Sci.*, **119**, 94-101. https://doi.org/10.1016/j.jafrearsci.2016.03.017.

Rybacki, E., Meier, T. and Dresen, G. (2016), "What controls the mechanical properties of shale rocks?-Part II: Brittleness", *J. Pet. Sci. Eng.*, **144**, 39-58. https://doi.org/10.1016/j.petrol.2016.02.022

Steffler, E.D., Epstein, J.S. and Conley, E.G. (2003), "Energy partitioning for a crack under remote shear and compression", *Int. J. Fract.*, **120**(4), 563-580. https://doi.org/10.1023/A:1025511703698.

Ulusay, R. (2015), *The ISRM Suggested Methods for Rock Characterization Testing and Monitoring 2007–2014*, Springer, Cham., Switzerland.

Wang, J.A. and Park, H.D. (2001), "Comprehensive prediction of rockburst based on analysis of strain energy in rocks", *Tunn. Undergr. Space Technol.*, **16**(1), 49-57. https://doi.org/10.1016/S0886-7798(01)00030-X.

Xie, H.P., Wang, J.A. and Qan, P.G. (1996), "Fractal characters of micropore evolution in marbles", *Phys. Lett. A*., **218**(3-6), 275-280. https://doi.org/10.1016/0375-9601(96)00390-8.

Yagiz, S. (2009), "Assessment of brittleness using rock strength and density with punch penetration test", *Tunn. Undergr. Space Technol*., **24**(1), 66-74. https://doi.org/10.1016/j.tust.2008.04.002.

Zhou, C.T., Zhang, K., Wang, H.B., Xu, Y.X. and Afraei, S. (2020), "A plastic strain based statistical damage model for brittle to ductile behaviour of rocks", *Geomech. Eng*., **21**(4), 349-356. https://doi.org/10.12989/gae.2020.21.4.349.

GC